Proc. Budapest'02 Workshop on
Quark & Hadron Dynamics (2002) 000–000

Budapest'02 Workshop on
Quark & Hadron Dynamics
Budapest, Hungary
March 3–7, 2002

The $\pi N \to e^+e^-N$ reaction close to the vector meson production threshold [a]

Madeleine Soyeur[1], Matthias F.M. Lutz[2] and Bengt Friman[2]

[1] DAPNIA/SPhN, CEA/Saclay, F-91191 Gif-sur-Yvette Cedex, France

[2] GSI, Planckstrasse 1, D-64291 Darmstadt, Germany
Institut für Kernphysik, TU Darmstadt, D-64289 Darmstadt, Germany

Abstract. The $\pi^-p \to e^+e^-n$ and $\pi^+n \to e^+e^-p$ reaction cross sections are calculated below and in the vicinity of the vector meson (ρ^0, ω) production threshold. These processes are largely responsible for the emission of e^+e^- pairs in pion-nucleus reactions and contribute to the dilepton spectra observed in relativistic heavy ion collisions. They are dominated by the decay of low-lying baryon resonances into vector meson-nucleon channels. The vector mesons materialize subsequently into e^+e^- pairs. Using $\pi N \to \rho^0 N$ and $\pi N \to \omega N$ amplitudes calculated in the center of mass energy interval $1.4 < \sqrt{s} < 1.8$ GeV, we compute the $\pi^-p \to e^+e^-n$ and $\pi^+n \to e^+e^-p$ reaction cross sections in these kinematics. Below the vector meson production threshold, the $\rho^0 - \omega$ interference in the e^+e^- channel appears largely destructive for the $\pi^-p \to e^+e^-n$ cross section and constructive for the $\pi^+n \to e^+e^-p$ cross section. The pion beam and the HADES detector at GSI offer a unique possibility to measure these effects. Such data would provide strong constraints on the coupling of vector meson-nucleon channels to low-lying baryon resonances.

Keywords: Vector meson production; Baryon resonances; Dileptons
PACS: 13.20; 13.75.G; 14.20.G

1. Introduction

The study of the $\pi^-p \to e^+e^-n$ and $\pi^+n \to e^+e^-p$ processes described in this work [1] aims at gaining understanding of the $\pi N \to \rho^0 N$ and $\pi N \to \omega N$ scattering amplitudes for center of mass energies close and below the vector meson production threshold ($1.5 < \sqrt{s} < 1.8$ GeV) [2]. There are well-known baryon resonances in this energy range, which contribute to the $\pi^-p \to e^+e^-n$ and $\pi^+n \to e^+e^-p$ scattering

a. This talk is based on the work published in Ref. [1].

amplitudes through their coupling to the πN, $\rho^0 N$ and ωN channels. These amplitudes involve in addition significant non-resonant processes. The phenomenological $\rho N N^*$ and $\omega N N^*$ coupling strengths needed to understand the data related to the $\pi N \to \rho^0 N$ and $\pi N \to \omega N$ amplitudes are pivotal quantities for baryon structure studies [2].

The exclusive observation of neutral vector mesons through their e^+e^- decay presents definite advantages over their observation through final states involving pions. Firstly, there are no competing processes, such as $\pi\Delta$ production which leads to the same $\pi\pi N$ final state and impairs consequently the identification of the ρ-meson in that channel. Secondly, both the ρ^0- and ω-mesons decay into the e^+e^- channel. This leads to a quantum interference pattern which is expected to reflect sensitively the structure and relative sign of the $\pi N \to \rho^0 N$ and $\pi N \to \omega N$ scattering amplitudes.

A proper understanding of the $\pi^- p \to e^+e^- n$ and $\pi^+ n \to e^+e^- p$ reactions appears also as a necessary step towards a detailed interpretation of the production of lepton pairs off nuclei induced by charged pions. Such reactions would be particularly sensitive to the propagation of ω-mesons in nuclei [3].

In Section 2, we present the relativistic coupled-channel model [2] used to describe the $\pi N \to \rho^0 N$ and $\pi N \to \omega N$ amplitudes and outline the calculation of the $\pi^- p \to e^+e^- n$ and $\pi^+ n \to e^+e^- p$ cross sections in the Vector Meson Dominance model. Our numerical results for these cross sections are displayed in Section 3. We discuss the $\rho^0 - \omega$ quantum interference pattern in the e^+e^- spectrum for both the $\pi^- p \to e^+e^- n$ and $\pi^+ n \to e^+e^- p$ reactions. We conclude briefly in Section 4.

2. Calculation of the $\pi^- p \to e^+e^- n$ and $\pi^+ n \to e^+e^- p$ cross sections close to the vector meson production threshold

We describe the $\pi N \to e^+e^- N$ reaction for e^+e^- pair invariant masses ranging from $\sim$0.4 to $\sim$0.8 GeV. Assuming Vector Meson Dominance for the electromagnetic current [5], the $\pi N \to \rho^0 N$ and $\pi N \to \omega N$ amplitudes are the basic quantities entering the calculation of the $\pi N \to e^+e^- N$ cross section. This assumption is illustrated in Fig. 1, where we show the diagrams contributing to the $\pi^- p \to e^+e^- n$ process.

We use the $\pi N \to \rho^0 N$ and $\pi N \to \omega N$ amplitudes obtained in the recent relativistic and unitary coupled-channel approach to meson-nucleon scattering of Ref. [2]. The available data on pion-nucleon elastic and inelastic scattering and on meson photoproduction off nucleon targets are fitted in the energy window $1.4 < \sqrt{s} < 1.8$ GeV, using an effective Lagrangian with quasi-local two-body meson-baryon interactions and a generalized form of Vector Meson Dominance to describe the coupling of vector mesons to real photons. The scheme comprises the πN, $\pi\Delta$, ρN, ωN, $K\Lambda$, $K\Sigma$ and ηN hadronic channels. The coupling constants entering the effective Lagrangian are parameters which are adjusted to reproduce the data. In view of the kinematics, only s-wave scattering in the ρN and ωN channels is

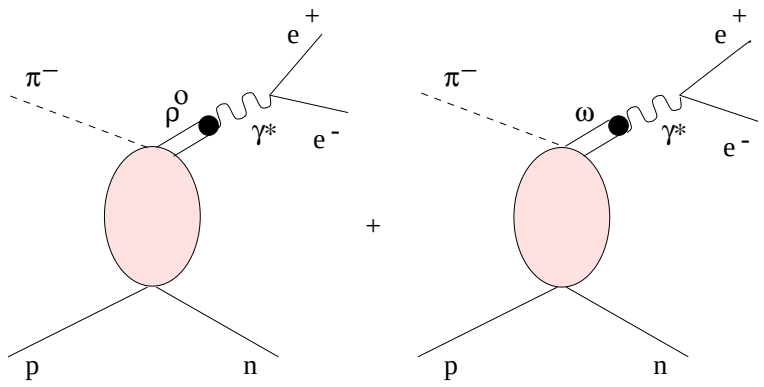

Fig. 1. Diagrams contributing to the $\pi^- p \to e^+e^- n$ amplitude with intermediate ρ^0- and ω-mesons.

included, restricting πN and $\pi\Delta$ scattering to s- and d-waves. The pion-nucleon resonances in the S_{11}, S_{31}, D_{13} and D_{33} partial waves are generated dynamically by solving Bethe-Salpeter equations [2]. In the $\rho^0 N$- and ωN-channels, the restriction to s-wave scattering means that the model applies to situations where the vector meson is basically at rest with respect to the scattered nucleon ($\sqrt{s} \simeq M_N + M_V$). This assumption implies that the range of validity of the present calculation is limited to e^+e^- pairs with invariant masses $m_{e^+e^-}$ close to ($\sqrt{s} - M_N$) and to values of $\sqrt{s}$ below and very close to threshold i.e. $1.5 < \sqrt{s} \leq 1.75$ GeV.

The $\pi N \to \rho N$ amplitude has isospin 1/2 and isospin 3/2 components while the $\pi N \to \omega N$ amplitude selects the isospin 1/2 channel. Both amplitudes have spin 1/2 and spin 3/2 parts.

The invariant transition matrix elements for the $\pi N \to \rho N$ and $\pi N \to \omega N$ reactions are given by

$$\begin{aligned}&\langle \rho^j(\overline{q})\, N(\overline{p})|\, \mathcal{T}\, |\pi^i(q)\, N(p)\rangle \\ &\qquad = (2\pi)^4\, \delta^4(q+\quad p-\overline{q}-\overline{p})\, \overline{u}(\overline{p})\, \epsilon^\mu(\overline{q})\, T^{ij}_{(\pi N\to\rho N)\,\mu}\, u(p), \end{aligned} \tag{1}$$

$$\begin{aligned}&\langle \omega(\overline{q})\, N(\overline{p})|\, \mathcal{T}\, |\pi^i(q)\, N(p)\rangle \\ &\qquad = (2\pi)^4\, \delta^4(q+\quad p-\overline{q}-\overline{p})\, \overline{u}(\overline{p})\, \epsilon^\mu(\overline{q})\, T^{i}_{(\pi N\to\omega N)\,\mu}\, u(p), \end{aligned} \tag{2}$$

where $T^{ij}_{(\pi N\to\rho N)\,\mu}$ and $T^{i}_{(\pi N\to\omega N)\,\mu}$ are functions of the three kinematic variables $w = p + q = \overline{p} + \overline{q}$ ($\sqrt{w^2} = \sqrt{s}$), q and $\overline{q}$. These scattering amplitudes can be

decomposed into isospin invariant components as

$$T^{ij}_{(\pi N\to\rho N)\,\mu}(\overline{q},q;w) \;=\sum_I T^{(I)}_{(\pi N\to\rho N)\,\mu}(\overline{q},q;w)\,P^{(I)\,ij}_{(\rho)}, \tag{3}$$

$$T^{i}_{(\pi N\to\omega N)\,\mu}(\overline{q},q;w) \;=\sum_I T^{(I)}_{(\pi N\to\omega N)\,\mu}(\overline{q},q;w)P^{(I)\,i}_{(\omega)}, \tag{4}$$

in which $P^{(I)\,ij}_{(\rho)}$ and $P^{(I)\,i}_{(\omega)}$ are isospin projectors [1]. The isospin invariant amplitudes can be expanded further into components of total angular momentum,

$$\begin{aligned} T^{(I)}_{(\pi N\to V N)\,\mu}(\overline{q},q;w) \;&=\; M^{(I,J=\frac{1}{2})}_{\pi N\to V N}(s)\; Y_{(J=\frac{1}{2})\,\mu}(\overline{q},q;w) \\ &+ M^{(I,J=\frac{3}{2})}_{\pi N\to V N}(s)\; Y_{(J=\frac{3}{2})\,\mu}(\overline{q},q;w). \end{aligned} \tag{5}$$

V stands for ρ or ω and $Y_{(J=\frac{1}{2})\,\mu}(\overline{q},q;w)$ and $Y_{(J=\frac{3}{2})\,\mu}(\overline{q},q;w)$ are relativistic angular momentum projectors [1].

The $\pi N\to\rho N$ and $\pi N\to\omega N$ amplitudes in the S_{11}, S_{31}, D_{13} and D_{33} channels obtained in Ref. [2] are displayed in Figs. 2 and 3. The quantities shown are the amplitudes $M^{(I,J)}_{\pi N\to\rho N}(s)$ and $M^{(I,J)}_{\pi N\to\omega N}(s)$ defined by Eq. (5), which depend only on the center of mass energy $\sqrt{s}$.

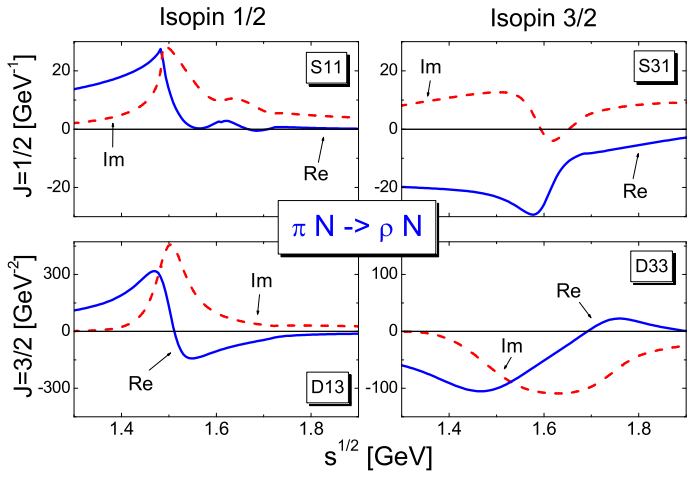

Fig. 2. Real and imaginary parts of the $\pi N\to\rho^0 N$ amplitudes in the pion-nucleon S_{11}, S_{31}, D_{13} and D_{33} partial waves [1].

The coupling to subthreshold resonances is clearly exhibited in these pictures. In the S_{11} channel, the N(1535) and the N(1650) resonances lead to peak structures in the imaginary parts of the amplitudes. The pion-induced ω production amplitudes in the D_{13} channel reflect the strong coupling of the N(1520) resonance to the ωN channel. The $\pi^- p \to \rho^0 n$ and $\pi^- p \to \omega n$ amplitudes are obtained from the

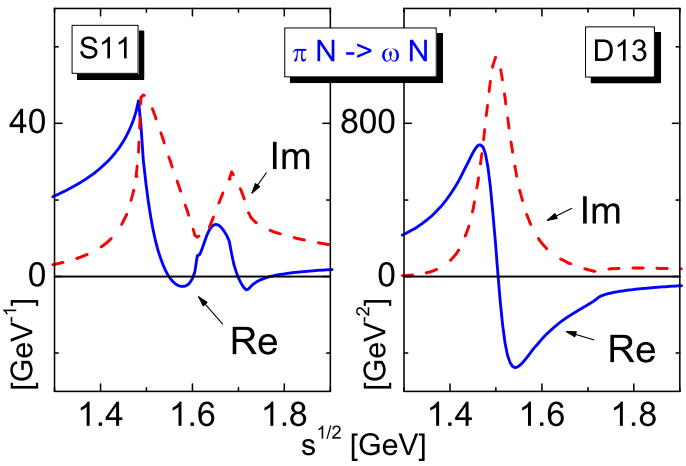

Fig. 3. Real and imaginary parts of the $\pi N \to \omega N$ amplitudes in the pion-nucleon S_{11} and D_{13} partial waves [1].

isospin 1/2 and isospin 3/2 scattering amplitudes by the relations,

$$M^J_{\pi^- p\to\rho^0 n} = -\frac{\sqrt{2}}{3} M^{(1/2,J)}_{\pi N\to\rho N} + \frac{\sqrt{2}}{3} M^{(3/2,J)}_{\pi N\to\rho N}, \tag{6}$$

$$M^J_{\pi^- p\to\omega n} = \sqrt{\frac{2}{3}} M^{(1/2,J)}_{\pi N\to\omega N}. \tag{7}$$

Similarly the $\pi^+ n \to \rho^0 p$ and $\pi^+ n \to \omega p$ amplitudes are given by

$$M^J_{\pi^+ n\to\rho^0 p} = \frac{\sqrt{2}}{3} M^{(1/2,J)}_{\pi N\to\rho N} - \frac{\sqrt{2}}{3} M^{(3/2,J)}_{\pi N\to\rho N}, \tag{8}$$

$$M^J_{\pi^+ n\to\omega p} = \sqrt{\frac{2}{3}} M^{(1/2,J)}_{\pi N\to\omega N}. \tag{9}$$

The phases of the isospin coefficients appearing in Eqs. (6) and (8) play a crucial role in determining the $\rho^0 - \omega$ interference in the $\pi^- p \to e^+ e^- n$ and $\pi^+ n \to e^+ e^- p$ reaction cross sections. The real and imaginary parts of the $\pi^- p \to \omega n$ and of the $\pi^+ n \to \omega p$ amplitudes are the same and mostly positive. In contrast, the $\pi^- p \to \rho^0 n$ and $\pi^+ n \to \rho^0 p$ amplitudes have opposite signs. The $\pi^- p \to \rho^0 n$ amplitudes are predominantly negative and will therefore interfere destructively with the $\pi^- p \to \omega n$ amplitudes. The $\pi^+ n \to \rho^0 p$ and $\pi^+ n \to \omega p$ amplitudes have the same sign over a large $\sqrt{s}$ interval, leading to a constructive interference.

The $\pi^- p \to e^+ e^- n$ and $\pi^+ n \to e^+ e^- p$ cross sections are calculated from the $\pi^- p \to \rho^0 n$, $\pi^- p \to \omega n$, $\pi^+ n \to \rho^0 p$ and $\pi^+ n \to \omega p$ amplitudes, assuming Vector Meson Dominance of the electromagnetic current [4, 5]. This assumption can be enforced in the effective Lagrangian by introducing vector meson-photon interaction terms of the form,

$$\mathcal{L}_{\gamma\mathcal{V}}^{\rangle\backslash\sqcup} \;=\; \frac{f_\rho}{2M_\rho^2} F^{\mu\nu}\, \rho^0_{\mu\nu} \;+\; \frac{f_\omega}{2M_\omega^2} F^{\mu\nu}\, \omega_{\mu\nu}, \tag{10}$$

where the photon and vector meson field tensors are defined by

$$F^{\mu\nu} \;=\; \partial^\mu A^\nu - \partial^\nu A^\mu, \tag{11}$$

$$V^{\mu\nu} \;=\; \partial^\mu V^\nu - \partial^\nu V^\mu. \tag{12}$$

In equation (10), M_ρ and M_ω are the ρ- and ω-masses and f_ρ and f_ω are dimensional coupling constants. Their magnitude can be determined from the e^+e^- partial decay widths of the ρ- and ω-mesons to be [6]

$$|f_\rho| = 0.036\, GeV^2, \tag{13}$$

$$|f_\omega| = 0.011\, GeV^2. \tag{14}$$

The relative sign of f_ρ and f_ω is fixed by vector meson photoproduction amplitudes [2]. We assume that the phase correlation between isoscalar and isovector currents is identical for real and virtual photons as in Sakurai's realization of the Vector Meson Dominance assumption [4]. With the conventions used in this paper, both f_ρ and f_ω are positive.

3. Numerical results

With the $\pi N \to \rho N$ and $\pi N \to \omega N$ amplitudes and the Vector Meson Dominance assumption discussed in Section 2, we have calculated the differential cross section $\frac{d\sigma}{d\overline{q}^2}_{\pi N \to e^+e^- N}$ for the $\pi^- p \to e^+ e^- n$ and $\pi^+ n \to e^+ e^- p$ reactions. The magnitude of the 4-vector $\overline{q}$ is the invariant mass $\mathrm{m}_{e^+e^-}$ of the e^+e^- pair. We refer to [1] for calculational details.

The differential cross sections for the $\pi^-p \to e^+e^-n$ and the $\pi^+n \to e^+e^-p$ reactions are computed for values of the total center of mass energy $\sqrt{s}$ ranging from 1.5 GeV up to 1.75 GeV. We explore the dependence of the $\rho^0 - \omega$ interference pattern in the e^+e^- channel on $\sqrt{s}$ in this energy range, in particular in the vicinity of the ω-meson production threshold ($\sqrt{s}$=1.72 GeV). We illustrate our results below threshold by displaying in Figs. 4 and 5 the differential cross sections for the $\pi^-p \to e^+e^-n$ and the $\pi^+n \to e^+e^-p$ reactions at $\sqrt{s}$=1.5 GeV, where the N(1520) and N(1535) baryon resonances play a dominant role. These figures show very clearly the isospin effects discussed in Section 2. For the two reactions, the ω and ρ^0 contributions to the cross section are the same. The ρ^0-ω interference is destructive for the $\pi^-p \to e^+e^-n$ reaction and constructive for the $\pi^+n \to e^+e^-p$ process. Consequently, the $\pi^-p \to e^+e^-n$ differential cross section is extremely small in the range of invariant masses considered in this calculation. In contrast, the constructive ρ^0-ω interference for the $\pi^+n \to e^+e^-p$ reaction leads to a sizeable differential cross section. This is a very striking prediction, linked to the resonant structure of the scattering amplitudes $M^{1/2}_{\pi N \to VN}$ and $M^{3/2}_{\pi N \to VN}$. Data on differential cross sections for the $\pi^-p \to e^+e^-n$ and $\pi^+n \to e^+e^-p$ reactions at $\sqrt{s}$=1.5 GeV would be very useful for making progress in the understanding of the couplings of both the N(1520) and N(1535) baryon resonances to the vector meson-nucleon channels.

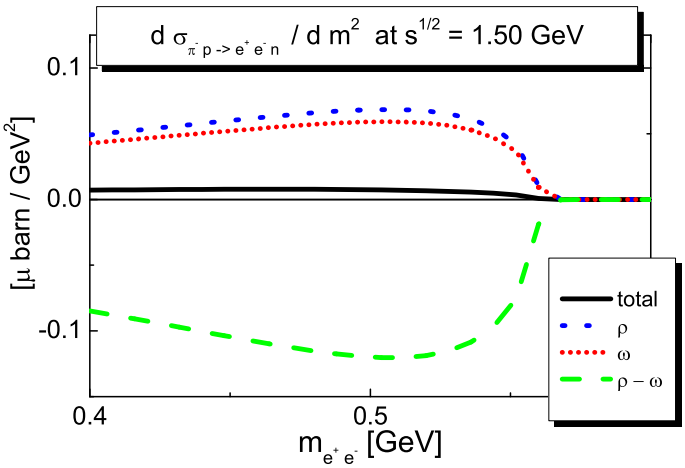

Fig. 4. Differential cross section for the $\pi^-p \to e^+e^-n$ reaction at $\sqrt{s}$=1.5 GeV as function of the invariant mass of the e^+e^- pair. The ρ^0 and the ω contributions are indicated by short-dashed and dotted lines respectively. The long-dashed line shows the $\rho^0 - \omega$ interference. The solid line is the sum of the three contributions.

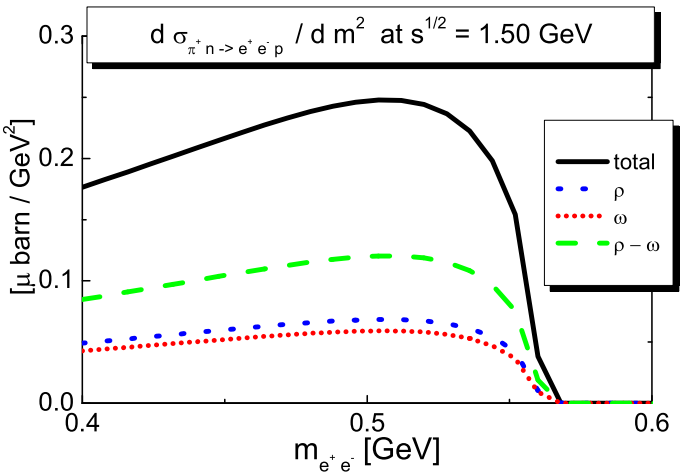

Fig. 5. Differential cross section for the $\pi^+ n \to e^+e^- p$ reaction at $\sqrt{s}$=1.5 GeV as function of the invariant mass of the e^+e^- pair. The ρ^0 and the ω contributions are indicated by short-dashed and dotted lines respectively. The long-dashed line shows the $\rho^0 - \omega$ interference. The solid line is the sum of the three contributions.

The differential cross sections for the $\pi^- p \to e^+e^- n$ and $\pi^+ n \to e^+e^- p$ reactions below threshold have been calculated also at $\sqrt{s}$=1.55, 1.60, 1.65 and 1.70 GeV [1]. The cross sections vary smoothly with the total center of mass energy. They exhibit the features discussed for $\sqrt{s}$=1.5 GeV, reflecting however dynamics associated with higher-lying resonances. Just below threshold ($\sqrt{s}$=1.70 GeV), the ω-contribution begins to increase, while the general features of the e^+e^- production in the two isospin channels remain the same.

The interference pattern changes drastically above the ω-meson threshold. Figs. 6 and 7 show the $\pi^- p \to e^+e^- n$ and $\pi^+ n \to e^+e^- p$ differential cross sections at $\sqrt{s}$=1.75 GeV. At this energy, the differential cross sections for the $\pi^- p \to e^+e^- n$ and $\pi^+ n \to e^+e^- p$ reactions are completely dominated by the ω-contribution. The magnitudes of the cross sections for the two reactions are comparable. The $\rho^0 - \omega$ interference is still destructive in the $\pi^- p \to e^+e^- n$ channel and constructive in the $\pi^+ n \to e^+e^- p$ channel, albeit very small. In both reactions, crossing the ω-production threshold leads to a sharp increase in the cross section, by two orders of magnitude in the $\pi^- p \to e^+e^- n$ channel and by one order of magnitude in the $\pi^+ n \to e^+e^- p$ channel.

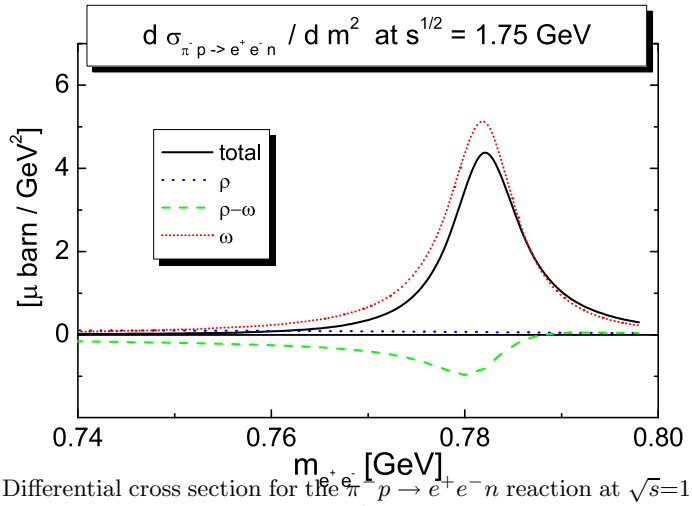

Fig. 6. Differential cross section for the $\pi^- p \to e^+e^-n$ reaction at $\sqrt{s}$=1.75 GeV as function of the invariant mass of the e^+e^- pair.

4. Conclusion

We have computed the e^+e^- pair invariant mass distributions for the $\pi^-p \to e^+e^-n$ and $\pi^+n \to e^+e^-p$ reactions below and close to the vector meson production threshold. We took as input the $\pi N \to \rho^0 N$ and $\pi N \to \omega N$ amplitudes obtained in a recent relativistic and unitary coupled-channel approach to meson-nucleon scattering [2]. Using the Vector Meson Dominance assumption, we have shown that the differential cross sections for the $\pi^-p \to e^+e^-n$ and $\pi^+n \to e^+e^-p$ reactions below the ω-threshold are very sensitive to the coupling of low-lying baryon resonances to vector meson-nucleon final states contributing to the ρ^0- and ω-meson production amplitudes. We find that the $\rho^0 - \omega$ interference is destructive in the $\pi^-p \to e^+e^-n$ channel and constructive in the $\pi^+n \to e^+e^-p$ channel (see also Ref. [7]). We predict a very small cross section for the $\pi^-p \to e^+e^-n$ reaction below threshold and a sizeable cross section for the $\pi^+n \to e^+e^-p$ reaction in this energy range. Above the ω-meson production threshold, both cross sections are comparable and much larger.

The magnitude of the $\pi^-p \to e^+e^-n$ and $\pi^+n \to e^+e^-p$ differential cross sections below the ω-threshold depends strongly on the structure and dynamics of baryon resonances. These reactions deserve experimental studies. Such a programme could be carried at GSI (Darmstadt) using the available pion beam and the HADES spectrometer [3]. These measurements would provide a necessary step towards the understanding of e^+e^- pair production in pion-nucleus reactions and in general significant constraints on the propagation of vector mesons in the nuclear medium.

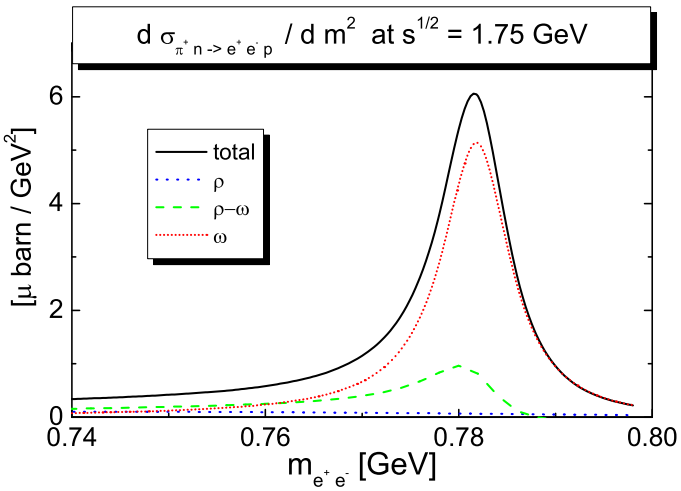

Fig. 7. Differential cross section for the $\pi^+ n \to e^+ e^- p$ reaction at $\sqrt{s}$=1.75 GeV as function of the invariant mass of the $e^+ e^-$ pair.

References

1. M.F.M. Lutz, B. Friman and M. Soyeur, nucl-th/0202049.
2. M.F.M. Lutz, Gy. Wolf and B. Friman, nucl-th/0112052.
3. W. Schön et al., Acta Physica Polonica B 27 (1996) 2959.
4. J.J. Sakurai, Currents and Mesons, The University of Chicago Press, 1969.
5. N.M. Kroll, T.D. Lee and B. Zumino, Phys. Rev. 157 (1967) 1376.
6. B. Friman and M. Soyeur, Nucl. Phys. A 600 (1996) 477.
7. A.I. Titov and B. Kämpfer, Eur. Phys. J. A. 12 (2001) 217.